

Article

# H<sub>2</sub>O·HF@C<sub>70</sub>: Encapsulation Energetics and Thermodynamics

Zdeněk Slanina <sup>1,2,\*</sup>, Filip Uhlík <sup>3</sup>, Xing Lu <sup>2</sup>, Takeshi Akasaka <sup>2</sup> and Ludwik Adamowicz <sup>1</sup><sup>1</sup> Department of Chemistry and Biochemistry, University of Arizona, Tucson, AZ 85721-0041, USA<sup>2</sup> State Key Laboratory of Materials Processing and Die & Mould Technology, School of Material Science and Engineering, Huazhong University of Science and Technology, Wuhan 430074, China<sup>3</sup> Department of Physical and Macromolecular Chemistry, Faculty of Science, Charles University, Albertov 6, 128 43 Praha 2, Czech Republic

\* Correspondence: zdeneks@email.arizona.edu

**Abstract:** This report deals with the quantum-chemical evaluation of the energetics and thermodynamics of the simultaneous encapsulation of HF and H<sub>2</sub>O by the IPR (isolated pentagon rule) C<sub>70</sub> fullerene cage, yielding H<sub>2</sub>O·HF@C<sub>70</sub> species which were synthesized and characterized recently, thus further expanding the family of fullerene endohedrals with non-metallic encapsulates. The structures were optimized at the DFT (density functional theory) M06-2X/6-31++G\*\* level. The encapsulation energetics were further refined by the advanced B2PLYPD/6-31++G\*\* and B2PLYPD/6-311++G\*\* methods. After enhancement of the B2PLYPD/6-311++G\*\* encapsulation energy for the BSSE and steric corrections, the encapsulation energy gain was obtained, as 26 kcal/mol. The equilibrium encapsulation thermodynamics were described using the M06-2X/6-31++G\*\* partition functions. The results correspond to our previous evaluations for the water dimer encapsulation by C<sub>84</sub> cages.

**Keywords:** endohedral; fullerene; metallofullerene; stability

## 1. Introduction

In addition to metal encapsulations yielding metallofullerenes, it is also possible for non-metals, and even small non-metallic molecules, to be encapsulated by fullerene cages. Metallofullerenes themselves are stabilized via charge transfer of up to four electrons from the metal to the cage. Such strong charge transfer and stabilization, primarily via Coulombic interactions, does not occur with non-metal encapsulation. The stabilization of non-metallic molecules is based [1] on non-bonding, in particular van der Waals interactions. N<sub>2</sub>@C<sub>60</sub> and N<sub>2</sub>@C<sub>70</sub> primarily represent such endohedrals that encapsulate non-metal molecules, prepared [2] by heating under high pressure. N<sub>2</sub>@C<sub>60</sub> has also been observed [3] in chromatographic separation after nitrogen ion implantation, otherwise primarily yielding N@C<sub>60</sub> [4–9]. Complexes of fullerenes with rare gas atoms [10–14] can also be prepared using [10] high temperatures, high pressures, and a catalyst [13]. A new, elegant encapsulation method for non-metallic molecules—such as molecular hydrogen molecules [15] and water molecules [16]—places the species inside open-cage fullerenes, and then closes the cage window synthetically [17,18]. Multi-step synthesis has even produced [19] (H<sub>2</sub>O)<sub>2</sub>@C<sub>70</sub>. Carbon monoxide [20,21] and H<sub>2</sub>O<sub>2</sub> [22,23] have also been placed inside open-cage C<sub>60</sub> derivatives.

Fullerene encapsulations of non-metal species have also been computed [24–42]: for example, the lowest-energy N<sub>2</sub>@C<sub>60</sub> structure that has been identified [28] is the N<sub>2</sub> unit, which is oriented towards a pair of parallel pentagons, so that the complex exhibits D<sub>5d</sub> symmetry. This type of minimum energy structure has also been computed [26] for NH<sub>3</sub>@C<sub>60</sub>. With N<sub>2</sub>@C<sub>60</sub> [28], the MP2 = FC/6-31G\* encapsulation energies, before and after the so-called basis set superposition error (BSSE) correction, are equal to –17.5 kcal/mol and –9.28 kcal/mol, respectively. The BSSE-corrected MP2 = FC/6-31G\* value for NH<sub>3</sub>@C<sub>60</sub> is [26] –5.23 kcal/mol. Once the corresponding entropy change ΔS<sub>T</sub><sup>0</sup> is evaluated, one can



**Citation:** Slanina, Z.; Uhlík, F.; Lu, X.; Akasaka, T.; Adamowicz, L. H<sub>2</sub>O·HF@C<sub>70</sub>: Encapsulation Energetics and Thermodynamics. *Inorganics* **2023**, *11*, 123. <https://doi.org/10.3390/inorganics11030123>

Academic Editor: Pingwu Du

Received: 19 February 2023

Revised: 27 February 2023

Accepted: 11 March 2023

Published: 15 March 2023



**Copyright:** © 2023 by the authors. Licensee MDPI, Basel, Switzerland. This article is an open access article distributed under the terms and conditions of the Creative Commons Attribution (CC BY) license (<https://creativecommons.org/licenses/by/4.0/>).

deal with the thermodynamics-controlling Gibbs energy term  $\Delta G_T^0$ . Using the partition functions from the DFT calculations, and the enthalpy terms derived from the BSSE-corrected MP2 = FC/6-31\* stabilization energy, the  $\Delta G_T^0$  standard changes for productions of  $N_2@C_{60}$  and  $NH_3@C_{60}$  at room temperature [26,28] read  $-2.64$  and  $1.53$  kcal/mol, respectively. Such stability evaluations have also been performed for water dimer and trimer encapsulations, in particular by the  $D_2(22)-C_{84}$  cage [36–39]. For example, when the encapsulation energy for the cyclic water-trimer encapsulation by  $D_2(22)-C_{84}$  was computed at the M06-2X/6-31++G\*\* level with the BSSE correction, it was found that the trimer storage in  $C_{84}$  yielded a potential-energy gain of 10.4 kcal/mol. The encapsulated trimer could have two different forms: either the conformation known for the free-gas-phase water trimer (*trans*,  $C_1$  symmetry) or the arrangement with the three non-hydrogen-bonded H atoms on the same side of the OOO plane (*cis*,  $C_3$  symmetry). The latter endohedral isomer was calculated [41] as lower in potential energy, by 0.071 kcal/mol, and formed about 57% of the equilibrium mixture at room temperature. The mentioned examples show that quantum-chemical calculations can productively complement observations of the non-metallic fullerene endohedrals.

This report continues the computational research line, and deals with quantum-chemical evaluation of the energetics and thermodynamics of the encapsulation of HF and  $H_2O$  into the IPR (isolated pentagon rule)  $C_{70}$  fullerene cage, yielding  $H_2O \cdot HF@C_{70}$  species synthesized and characterized [43] recently. The calculations could possibly be applied in the organization of direct high-pressure preparation of the species used for other systems [10–14] (where a temporary cage window is created by a catalytic action).

## 2. Calculations

The calculations began with geometry optimizations, performed using the density functional theory (DFT) approach—namely, the M06-2X functional, tested recently [44]—as it is the most reliable approximation for numerous application situations, including long-range interactions, hydrogen bonds, thermochemistry, and kinetics. The M06-2X functional was applied here with the standard 6-31++G\*\* basis set [45] (i.e., the M06-2X/6-31++G\*\* treatment). In order to check the geometrical or physical nature of the stationary points localized on the M06-2X/6-31++G\*\* potential hypersurface, harmonic vibrational analysis was carried out, thus confirming that the local energy minima had been found. An ultrafine grid in numerical integrations of the DFT functional (or superfine grid for the endohedral, to improve the reliability of low frequencies), and a tight SCF convergence criterion, were used.

The encapsulation energetics were refined beyond the DFT level, in order to reliably describe the electron-correlation effects, namely using the B2PLYPD treatment [46] with a dispersion (D) correction, and considering all electrons (B2PLYPD = FU). The B2PLYPD approach is a relatively new method, representing the application of the original second-order Møller–Plesset (MP2) perturbation treatment [47] to DFT wavefunctions. The B2PLYPD treatment was performed here, in the the optimized M06-2X/6-31++G\*\* structures, using the 6-31++G\*\*, and also 6-311++G\*\* basis sets, i.e., B2PLYPD/6-31++G\*\* and B2PLYPD/6-311++G\*\* quantum-chemical levels. Moreover, the basis set superposition error (BSSE) was estimated by the Boys–Bernardi counterpoise (CP) method [48] (for a more detailed description, see Appendix A). The CP correction is only rarely considered [49–52] with fullerene species, though it can bring about significant energy changes. The BSSE-corrected values were still further improved here by the recently suggested [37,53] steric correction.

All the computations were carried out with the Gaussian 09 program package [54]. The computations were performed in a parallel regime, with up to 24 processors (up to 3 GHz each).

## 3. Results and Discussion

The M06-2X/6-31++G\*\* optimized structure of  $H_2O \cdot HF@C_{70}$  agreed with the observed results [43]. In particular, the observed hydrogen-bond length is 1.39 Å, while the

value calculated here was 1.481 Å. Similarly, the observed F-O distance is 2.438 Å, while the calculated one was 2.447 Å. The calculations treated a free, gas-phase  $\text{H}_2\text{O}\cdot\text{HF}@C_{70}$  species, while the X-ray experiment [43] dealt with a porphyrin cocrystal.

Table A1 reports the calculated encapsulation energetics. The presented potential-energy changes describe the gas-phase formation of  $\text{H}_2\text{O}\cdot\text{HF}@C_{70}$ , i.e., the equilibrium encapsulation processes,



connected with an encapsulation potential-energy change  $\Delta E_{enc}$ . The energy changes were always negative (Table A1), i.e., there was a gain in energy; the encapsulation process (1) is exothermic and, thus, convenient from the thermodynamic point of view. The calculated terms were rather similar in both considered basis sets. On the other hand, the M06-2X values differed significantly from the B2PLYPD ones. This situation can be interpreted as the M06-2X functional not having described sufficiently the electron-correlation effects in this type of system. Thus, the B2PLYPD terms should be preferred for the endohedrals. Hence, the B2PLYPD/6-311++G\*\* encapsulation energy value of  $-26.02$  kcal/mol was used for the thermodynamic treatment.

The energy terms presented in Table A1 include the BSSE correction evaluated in the so-called CP3 scheme [37,55], i.e., the association of three species (1). The Boys–Bernardi CP method [48] is still an approximative approach, introduced in order to ensure that each component of a chemical process is formally treated with the same number of basis-set functions. This formal unified description is achieved via so-called ghost atoms with no electrons. The BSSE problem originates in the finiteness of basis sets, and it should disappear in the rather hypothetical case of an infinite basis set. The BSSE correction is an important term—oligomerization energy gain would otherwise be overestimated [37,55] by several kcal/mol.

There is still another computational aspect related to the CP3 estimation of the BSSE term. The original Boys–Bernardi counterpoise method was suggested [48] for dimers handled with a fixed geometry (though the structures of the monomeric units differ in free and dimeric form). Although a fully BSSE-respecting geometry optimization would, in principle, be possible [56], it is feasible only for relatively simple systems. Nevertheless, in order to reflect the geometry distortion, a simpler, straightforward steric-corrected BSSE approach has recently been suggested [37,53] (for details, see Appendix A). In the conventional CP3 treatment, the geometries of the three sub-units ( $\text{H}_2\text{O}$ ,  $\text{HF}$ ,  $C_{70}$  in our case) are taken to be the same as in the whole complex ( $\text{H}_2\text{O}\cdot\text{HF}@C_{70}$ ), so that only four energy calculations are required, without any structure re-optimization. The steric-corrected BSSE treatment [37,53] goes a step further, as it includes the difference between the energy of the carbon-cage geometry simply taken from  $\text{H}_2\text{O}\cdot\text{HF}@C_{70}$  and the energy of the related fully-optimized empty  $C_{70}$  cage (which has to be slightly lower). Similar steric corrections are also computed for the  $\text{H}_2\text{O}$  and  $\text{HF}$  components. For simplicity, the steric corrections in this work were evaluated only at the M06-2X/6-31++G\*\* level. The gain in the encapsulation energy was in fact reduced by the steric correction at the M06-2X/6-31++G\*\* computational level, by some 1.49 kcal/mol (i.e., a somewhat larger reduction than that, for example, found [37] for the CP3 steric corrections with  $(\text{H}_2\text{O})_2@D_2(22)-C_{84}$  and  $(\text{H}_2\text{O})_2@D_{2d}(23)-C_{84}$ ).

The encapsulation energies  $\Delta E_{enc}$ , with the inclusion of the BSSE and steric corrections, are presented in Table A1. The B2PLYPD/6-311++G\*\* terms should be preferred in further considerations, as they represent the most sophisticated of the approaches considered here. Interestingly, the observed [57] dissociation energy of a free  $\text{H}_2\text{O}\cdot\text{HF}$  complex was also reproduced well by the B2PLYPD/6-311++G\*\* method. The encapsulation-energy gain for  $\text{H}_2\text{O}\cdot\text{HF}@C_{70}$  was somewhat larger than previously found, for example, with  $(\text{H}_2\text{O})_2@D_2(22)-C_{84}$  [37,38]. With future developments in computer technology, the B2PLYPD/6-311++G\*\* approach should, however, be tested at a still higher level of quantum-chemical methodology.

Let us note for completeness that, in addition to the CP3 scheme considered here for BSSE corrections, a simpler CP2 scheme was previously applied [37] to water-dimer encapsulation. While the CP3 scheme deals with three sub-units, as in the above reaction (1), the CP2 approach dealt simply with the encapsulation of the whole complex  $\text{H}_2\text{O}\cdot\text{HF}$  by the  $\text{C}_{70}$  cage. Generally speaking, the CP3 scheme should produce larger energy gains compared to the CP2 decomposition, owing to the additional stabilization energy originating in the encapsulate formation from the monomeric units.

The encapsulation potential energy change,  $\Delta E_{enc}$ , was enhanced, for the thermodynamic treatment, by the vibrational zero-point energy ZPE, leading to encapsulation enthalpy at absolute zero temperature  $\Delta H_{0,enc}^0$ :

$$\Delta H_{0,enc}^0 = \Delta E_{enc} + \Delta ZPE_{enc}. \quad (2)$$

Application of the heat content functions evaluated with the partition function treatment yielded the standard encapsulation enthalpy change, at temperature  $T$ :  $\Delta H_{T,enc}^0$ . The partition function treatment also produced the standard encapsulation entropy change, at temperature  $T$ :  $\Delta S_{T,enc}^0$ . Thus, we arrived at the standard encapsulation Gibbs energy change  $\Delta G_{T,enc}^0$ :

$$\Delta G_{T,enc}^0 = \Delta H_{T,enc}^0 - T\Delta S_{T,enc}^0. \quad (3)$$

The encapsulation equilibrium constant  $K_{p,enc}$  for reaction (1), expressed in the partial pressures  $p$  of the reaction components,

$$K_{p,enc} = \frac{p_{\text{H}_2\text{O}\cdot\text{HF@C}_{70}}}{p_{\text{H}_2\text{O}}p_{\text{HF}}p_{\text{C}_{70}}} \quad (4)$$

is related to the standard encapsulation Gibbs energy change  $\Delta G_{T,enc}^0$  by

$$\Delta G_{T,enc}^0 = -RT \ln K_{p,enc} \quad (5)$$

where  $R$  denotes the gas constant.

Table A2 presents the thermodynamic characteristics for the equilibrium process (1) at room temperature. Both terms,  $\Delta H_{T,enc}^0$  and  $\Delta G_{T,enc}^0$ , remained negative. As already noted with the simpler  $\Delta E_{enc}$  term, the encapsulation process (1) was exothermic and, thus, convenient from the thermodynamic point of view. The calculated  $\Delta G_{T,enc}^0$  value of  $-5.63$  kcal/mol (Table A2) was comparable to findings for water encapsulations by the  $\text{C}_{84}$  fullerene cages [36–39,41]. As in our previous computational evaluations of non-metallic fullerene endohedrals [26,28,36–41], the partition functions  $q_i$  were basically of the usual rigid rotor and harmonic oscillator (RRHO) quality [58] (as only was feasible with the presently available computer resources). In terms of the partition functions  $q_i$  and the encapsulation enthalpy at the absolute zero temperature  $\Delta H_{0,enc}^0$ , the encapsulation equilibrium constant  $K_{p,enc}$  (4) was given by a formula [58],

$$K_{p,enc} = \frac{\frac{q_{\text{H}_2\text{O}\cdot\text{HF@C}_{70}}^0}{N_A}}{\frac{q_{\text{H}_2\text{O}}^0}{N_A} \frac{q_{\text{HF}}^0}{N_A} \frac{q_{\text{C}_{70}}^0}{N_A}} \exp\left(-\frac{\Delta H_{0,enc}^0}{RT}\right), \quad (6)$$

where  $N_A$  denoted the Avogadro number. The form of relation (6) allowed for some convenient cancellation of the higher contributions [59] beyond the RRHO approximation. However, future efforts should deal with further improvements of the RRHO partition functions commonly employed [36–39,60] for encapsulation thermodynamics. Such developments should, in particular, deal with encapsulate motions, important not only for stability predictions but also for the cage symmetries effectively observed [18,61,62] as a consequence of the related observational time scales [58]. The symmetry issue is also closely related to the effective, dynamic symmetry numbers [38] in the rotational partition functions [63], an aspect that is important for all endohedrals, regardless of the encapsu-

late type: one option is to work with the so-called FEM approach [60], instead of RRHO partition functions (the two treatments can possibly suggest bounds for thermodynamic terms).

The encapsulation equilibrium constant in Table A2 was sensitive to the encapsulation enthalpy term  $\Delta H_{T,enc}^o$  as its related encapsulation enthalpy at the absolute zero temperature  $\Delta H_{0,enc}^o$  appeared in relation [6] in the exponential function: this aspect, in turn, highlights the importance of precise energy calculations.

#### 4. Conclusions

Our quantum-chemical evaluation of the energetics and thermodynamics of the simultaneous encapsulation of HF and H<sub>2</sub>O by the IPR C<sub>70</sub> fullerene cage further expands characterization of the relatively new family of fullerene endohedrals containing non-metallic encapsulates. The evaluations were carried out at the most advanced level presently applicable, yielding to the encapsulation-energy gain of 26 kcal/mol. Nevertheless, the results should in future be tested at still higher computational levels, such as the quadratic configuration interaction method, QCISD, or even the Gn theory [64], when allowed by computer resources. Further developments are also needed in the construction of the partition functions for thermodynamic evaluations, in order to somehow respect the anharmonic and non-rigid features of the endohedrals, though this step is also at present limited by the available computational power. The obtained estimate of the encapsulation equilibrium constant corresponded to the values previously derived [36–39,41] for the encapsulations of the water dimer by C<sub>84</sub> cages, and to other computed encapsulations [60]: the possibility is thus not excluded that even H<sub>2</sub>O·HF@C<sub>70</sub> could be prepared by direct catalytic high-pressure treatment [10–14]. Similar computational treatments of other fullerene systems with non-metallic encapsulates will offer a further insight into this newly established endohedral class, even having some application potential as a different approach to modifications of fullerene properties.

**Author Contributions:** The authors contributed equally to this article. All authors have read and agreed to the published version of the manuscript.

**Funding:** National Natural Science Foundation of China (21925104 and 92261204), the Hubei Provincial Natural Science Foundation of China (No. 2021CFA020), and the International Cooperation Key Project of Science and Technology Department of Shaanxi.

**Data Availability Statement:** Not applicable.

**Acknowledgments:** The reported research was supported by the Charles University Centre of Advanced Materials/CUCAM (CZ.02.1.01/0.0/0.0/15\_003/0000417), and by the MetaCentrum (LM2010005) and CERIT-SC (CZ.1.05/3.2.00/08.0144) computing facilities. The very initial phase of the research line was also supported by the Alexander von Humboldt-Stiftung and the Max Planck Institut für Chemie (Otto Hahn Institut).

**Conflicts of Interest:** The authors declare no conflict of interest.

#### Appendix A

Let us consider a general association process (regardless of the nature of the bonding types involved):



In the traditional approach, i.e., without the Boys–Bernardi counterpoise (CP) correction [48] (also called the BSSE correction), the reaction potential-energy change  $\Delta E_r$  is taken as the difference of the potential energies of the reaction components, straightforwardly evaluated in their own basis sets (indicated in the upper indexes):

$$\Delta E_{r,noCP} = E_C^{(C)} - E_A^{(A)} - E_B^{(B)}. \quad (\text{A2})$$

As the basis sets used in relation [8] are different, the three energy terms are not calculated at the same level; therefore, they are not consistent: thus, they are not strictly comparable or directly applicable.

In the CP-corrected treatment, the three reaction components are described by the same basis set, namely by the basis set of the product C:

$$\Delta E_{r,CP} = E_C^{(C)} - E_A^{(C)} - E_B^{(C)}. \quad (\text{A3})$$

As the basis set of C is larger than that of either A or B, there has to be energy decrease:  $E_A^{(C)} < E_A^{(A)}$ , and similarly  $E_B^{(C)} < E_B^{(B)}$  (potential energy decreases with increasing basis set). In other words, the absolute value of the reaction energy will also be reduced:  $|\Delta E_{r,CP}| < |\Delta E_{r,noCP}|$ . For example [37], for the water-dimer encapsulation by the  $D_2(22)$ - $C_{84}$  cage, the M06-2X/6-31++G\*\* potential-energy reaction change, without the CP2 correction, is  $-23.4$  kcal/mol, while with the CP2 correction the term changes to  $-19.2$  kcal/mol. Similarly [37], for the  $D_{2d}(23)$ - $C_{84}$  cage, the reaction change before the BSSE correction is  $-21.8$  kcal/mol, while after the BSSE correction the term amounts to  $-17.8$  kcal/mol.

Let us move to yet another correction. In the previous paragraph, the geometries of the two reactants A and B were simply taken from the optimized structure C. Now, the geometries of the free reactants will also be optimized. The additional step brings new energies for the reactants A and B (the new energies are somewhat lower, as geometry optimization means searching for a local energy minimum), denoted by *o* in the lower index,  $E_{A,o}^{(A)}$  and  $E_{B,o}^{(B)}$ . Hence, we can move to a steric-corrected term,

$$\Delta E_{r,noCP,o} = E_C^{(C)} - E_{A,o}^{(A)} - E_{B,o}^{(B)} \quad (\text{A4})$$

and subsequently to the steric correction  $\Delta E_{ster}$  itself:

$$\Delta E_{r,noCP,o} = \Delta E_{r,noCP} + \Delta E_{ster}. \quad (\text{A5})$$

In an approximation, the steric correction  $\Delta E_{ster}$  from relation (A5) is then straightforwardly used also for the improvement of the  $\Delta E_{r,CP}$  term. In the above example [37] of the water-dimer encapsulation by the  $D_2(22)$ - $C_{84}$  cage, the M06-2X/6-31++G\*\* potential-energy reaction change, with the CP2 correction of  $-19.2$  kcal/mol, amounts, after the steric correction, to  $-16.9$  kcal/mol. Similarly [37], for the  $D_{2d}(23)$ - $C_{84}$  cage, the reaction term is changed from  $-17.8$  kcal/mol to the final value of  $-14.4$  kcal/mol. The steric correction is positive, as the geometry optimizations still lower the energies of reactants A and B.

**Table A1.** The encapsulation energy  $\Delta E_{enc}$  for  $\text{H}_2\text{O}\cdot\text{HF}@C_{70}$ , calculated by selected approaches <sup>a</sup> and inclusion of the CP3 BSSE and steric corrections.

Calc. Level	$\Delta E_{enc}/\text{kcal}\cdot\text{mol}^{-1}$	
	6-31++G**	6-311++G**
M06-2X	-31.29	-31.79
B2PLYPD	-25.75	-26.02

<sup>a</sup> In the M062X/6-31++G\*\* optimized geometry, see Figure A1.

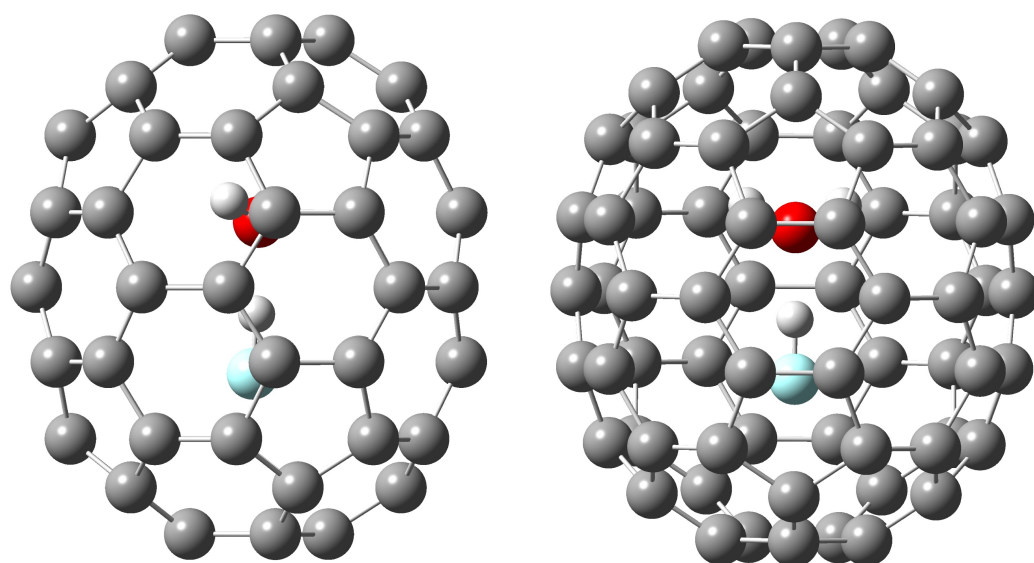


**Figure A1.** Two views of the M06-2X/6-31++G\*\* optimized structure of H<sub>2</sub>O·HF@C<sub>70</sub>.

**Table A2.** The standard <sup>a</sup> enthalpy  $\Delta H_{T,enc}^{\circ}$ , entropy  $T\Delta S_{T,enc}^{\circ}$ , Gibbs energy  $\Delta G_{T,enc}^{\circ}$  changes, and the equilibrium constants  $K_{p,enc}$  for the gas-phase equilibrium formation (1) of H<sub>2</sub>O·HF@C<sub>70</sub>, evaluated <sup>b</sup> at room temperature  $T = 298.15$  K.

	$\Delta H_{T,enc}^{\circ}$ (kcal/mol)	$T\Delta S_{T,enc}^{\circ}$ (kcal/mol)	$\Delta G_{T,enc}^{\circ}$ (kcal/mol)	$K_{p,enc}$ (atm <sup>-2</sup> )
B2PLYPD/6-311++G**	−23.24	−17.60	−5.63	$1.346 \times 10^4$

<sup>a</sup> The standard state—ideal gas phase at 1 atm = 101,325 Pa pressure. <sup>b</sup> The partition functions based on the M062X/6-31++G\*\* molecular characteristics.

## References

- Dresselhaus, M.S.; Dresselhaus, G.; Eklund, P.C. *Science of Fullerenes and Carbon Nanotubes*; Academic Press: San Diego, CA, USA, 1996; p. 316.
- Peres, T.; Cao, B.P.; Cui, W.D.; Khong, A.; Cross, R.J.; Saunders, M.; Lifshitz, C. Some new diatomic molecule containing endohedral fullerenes. *Int. J. Mass Spectr.* **2001**, *210/211*, 241–247. [[CrossRef](#)]
- Suetsuna, T.; Drago, N.; Harneit, W.; Weidinger, A.; Shimotani, H.; Ito, S.; Takagi, H.; Kitazawa, K. Separation of N<sub>2</sub>@C<sub>60</sub> and N@C<sub>60</sub>. *Chem. Eur. J.* **2002**, *8*, 5079–5083. [[CrossRef](#)] [[PubMed](#)]
- Murphy, T.A.; Pawlik, T.; Weidinger, A.; Höhne, M.; Alcalá, R.; Spaeth, J.-M. Observation of atomlike nitrogen in nitrogen-implanted solid C<sub>60</sub>. *Phys. Rev. Lett.* **1996**, *77*, 1075–1078. [[CrossRef](#)] [[PubMed](#)]
- Knapp, C.; Dinse, K.-P.; Pietzak, B.; Waiblinger, M.; Weidinger, A. Fourier transform EPR study of N@C<sub>60</sub> in solution. *Chem. Phys. Lett.* **1997**, *272*, 433–437. [[CrossRef](#)]
- Pietzak, B.; Waiblinger, M.; Murphy, T.A.; Weidinger, A.; Höhne, M.; Dietel, E.; Hirsch, A. Buckminsterfullerene C<sub>60</sub>: A chemical Faraday cage for atomic nitrogen. *Chem. Phys. Lett.* **1997**, *279*, 259–263. [[CrossRef](#)]
- Cao, B.P.; Peres, T.; Cross, R.J.; Saunders, M.; Lifshitz, C. Do nitrogen-atom-containing endohedral fullerenes undergo the shrink-wrap mechanism? *J. Phys. Chem. A* **2001**, *105*, 2142–2146. [[CrossRef](#)]
- Kobayashi, K.; Nagase, S.; Dinse, K.-P. A theoretical study of spin density distributions and isotropic hyperfine couplings of N and P atoms in N@C<sub>60</sub>, P@C<sub>60</sub>, N@C<sub>70</sub>, N@C<sub>60</sub>(CH<sub>2</sub>)<sub>6</sub>, and N@C<sub>60</sub>(SiH<sub>2</sub>)<sub>6</sub>. *Chem. Phys. Lett.* **2003**, *377*, 93–98. [[CrossRef](#)]
- Wakahara, T.; Matsunaga, Y.; Katayama, A.; Maeda, Y.; Kako, M.; Akasaka, T.; Okamura, M.; Kato, T.; Choe, Y.K.; Kobayashi, K.; et al. A comparison of the photochemical reactivity of N@C<sub>60</sub> and C<sub>60</sub>: Photolysis with disilirane. *Chem. Commun.* **2003**, *39*, 2940–2941. [[CrossRef](#)]
- Saunders, M.; Jiménez-Vázquez, H.A.; Cross, R.J.; Poreda, R.J. Stable compounds of helium and neon: He@C<sub>60</sub> and Ne@C<sub>60</sub>. *Science* **1993**, *259*, 1428–1430. [[CrossRef](#)]
- Saunders, M.; Jiménez-Vázquez, H.A.; Cross, R.J.; Mroczkowski, S.; Freedberg, D.I.; Anet, F.A.L. Probing the interior of fullerenes by <sup>3</sup>He NMR spectroscopy of endohedral <sup>3</sup>He@C<sub>60</sub> and <sup>3</sup>He@C<sub>70</sub>. *Nature* **1994**, *367*, 256–258. [[CrossRef](#)]
- Cross, R.J.; Saunders, M.; Prinzbach, H. Putting helium inside dodecahedrane. *Org. Lett.* **1999**, *1*, 1479–1481. [[CrossRef](#)]
- Cross, R.J.; Saunders, M. Catalyzed incorporation of noble gases in fullerenes. In *Recent Advances in the Chemistry and Physics of Fullerenes and Related Materials, Volume 11—Fullerenes for the New Millennium*; Kadish, K.M., Kamat, P.V., Guldi, D., Eds.; The Electrochemical Society: Pennington, NJ, USA, 2001; pp. 298–300.

14. Rubin, Y.; Jarrosson, T.; Wang, G.-W.; Bartberger, M.D.; Houk, K.N.; Schick, G.; Saunders, M.; Cross, R.J. Insertion of helium and molecular hydrogen through the orifice of an open fullerene. *Angew. Chem., Int. Ed. Engl.* **2001**, *40*, 1543–1546. [[CrossRef](#)]
15. Carravetta, M.; Murata, Y.; Murata, M.; Heinmaa, I.; Stern, R.; Tontcheva, A.; Samoson, A.; Rubin, Y.; Komatsu, K.; Levitt, M.H. Solid-state NMR spectroscopy of molecular hydrogen trapped inside an open-cage fullerene. *J. Am. Chem. Soc.* **2004**, *126*, 4092–4093. [[CrossRef](#)]
16. Iwamatsu, S.-I.; Uozaki, T.; Kobayashi, K.; Re, S.; Nagase, S.; Murata, S. A bowl-shaped fullerene encapsulates a water into the cage. *J. Am. Chem. Soc.* **2004**, *126*, 2668–2669. [[CrossRef](#)]
17. Komatsu, K.; Murata, M.; Murata, Y. Encapsulation of molecular hydrogen in fullerene C<sub>60</sub> by organic synthesis. *Science* **2005**, *307*, 238–240. [[CrossRef](#)]
18. Kurotobi, K.; Murata, Y. A single molecule of water encapsulated in fullerene C<sub>60</sub>. *Science* **2011**, *333*, 613–616. [[CrossRef](#)]
19. Zhang, R.; Murata, M.; Aharen, T.; Wakamiya, A.; Shimoaka, T.; Hasegawa, T.; Murata, Y. Synthesis of a distinct water dimer inside fullerene C<sub>70</sub>. *Nature Chem.* **2016**, *8*, 435–441. [[CrossRef](#)]
20. Iwamatsu, S.; Stanisky, C.M.; Cross, R.J.; Saunders, M.; Mizorogi, N.; Nagase, S.; Murata, S. Carbon monoxide inside an open-cage fullerene. *Angew. Chem. Intl. Ed.* **2006**, *45*, 5337–5340. [[CrossRef](#)]
21. Shi, L.J.; Yang, D.Z.; Colombo, F.; Yu, Y.M.; Zhang, W.X.; Gan, L.B. Punching a carbon atom of C<sub>60</sub> into its own cavity to form an endohedral complex CO@C<sub>59</sub>O<sub>6</sub> under mild conditions. *Chem. Eur. J.* **2013**, *19*, 16545–16549. [[CrossRef](#)]
22. Li, Y.; Lou, N.; Xu, D.; Pan, C.; Lu, X.; Gan, L. Oxygen-delivery materials: Synthesis of an open-cage fullerene derivative suitable for encapsulation of H<sub>2</sub>O<sub>2</sub> and O<sub>2</sub>. *Angew. Chem. Int. Ed.* **2018**, *57*, 14144–14148. [[CrossRef](#)]
23. Gan, L. Molecular containers derived from [60]fullerene through peroxide chemistry. *Acc. Chem. Res.* **2019**, *52*, 1793–1801. [[CrossRef](#)] [[PubMed](#)]
24. Cioslowski, J. Endohedral chemistry: Electronic structures of molecules trapped inside the C<sub>60</sub> cage. *J. Am. Chem. Soc.* **1991**, *113*, 4139–4141. [[CrossRef](#)]
25. Charkin, O.P.; Klimenko, N.M.; Charkin, D.O.; Mebel, A.M. Theoretical study of host-guest interaction in model endohedral fullerenes with tetrahedral molecules and ions of MH<sub>4</sub> hydrides inside the C<sub>60</sub>H<sub>36</sub>, C<sub>60</sub>H<sub>24</sub>, C<sub>84</sub>, and C<sub>60</sub> cages. *Russ. J. Inorg. Chem.* **2004**, *49*, 868–880.
26. Slanina, Z.; Uhlík, F.; Adamowicz, L.; Nagase, S. Computing fullerene encapsulation of non-metallic molecules: N<sub>2</sub>@C<sub>60</sub> and NH<sub>3</sub>@C<sub>60</sub>. *Mol. Simul.* **2005**, *31*, 801–806. [[CrossRef](#)]
27. Ramachandran, C.N.; Sathyamurthy, N. Water clusters in a confined nonpolar environment. *Chem. Phys. Lett.* **2005**, *410*, 348–351. [[CrossRef](#)]
28. Slanina, Z.; Nagase, S. A computational characterization of N<sub>2</sub>@C<sub>60</sub>. *Mol. Phys.* **2006**, *104*, 3167–3171. [[CrossRef](#)]
29. Shameema, O.; Ramachandran, C.N.; Sathyamurthy, N. Blue shift in X-H stretching frequency of molecules due to confinement. *J. Phys. Chem. A* **2006**, *110*, 2–4. [[CrossRef](#)]
30. Slanina, Z.; Pulay, P.; Nagase, S. H<sub>2</sub>, Ne, and N<sub>2</sub> energies of encapsulation into C<sub>60</sub> evaluated with the MPWB1K functional. *J. Chem. Theory Comput.* **2006**, *2*, 782–785. [[CrossRef](#)]
31. Mazurek, A.P.; Sadlej-Sosnowska, N. Is fullerene C<sub>60</sub> large enough to host an aromatic molecule? *Int. J. Quantum Chem.* **2011**, *111*, 2398–2405. [[CrossRef](#)]
32. Rodríguez-Forteza, A.; Balch, A.L.; Poblet, J.M. Endohedral metallofullerenes: A unique host-guest association. *Chem. Soc. Rev.* **2011**, *40*, 3551–3563. [[CrossRef](#)]
33. Varadwaj, A.; Varadwaj, P.R. Can a single molecule of water be completely isolated within the subnano-space inside the fullerene C<sub>60</sub> cage? A Quantum chemical prospective. *Chem. Eur. J.* **2012**, *18*, 15345–15360. [[CrossRef](#)]
34. Farimani, A.B.; Wu, Y.B.; Aluru, N.R. Rotational motion of a single water molecule in a buckyball. *Phys. Chem. Chem. Phys.* **2013**, *15*, 17993–18000. [[CrossRef](#)]
35. Popov, A.A.; Yang, S.; Dunsch, L. Endohedral fullerenes. *Chem. Rev.* **2013**, *113*, 5989–6113. [[CrossRef](#)]
36. Uhlík, F.; Slanina, Z.; Lee, S.-L.; Wang, B.-C.; Adamowicz, L.; Nagase, S. Water-dimer stability and its fullerene encapsulations. *J. Comput. Theor. Nanosci.* **2015**, *12*, 959–964. [[CrossRef](#)]
37. Slanina, Z.; Uhlík, F.; Lu, X.; Akasaka, T.; Lemke, K.H.; Seward, T.M.; Nagase, S.; Adamowicz, L. Calculations of the water-dimer encapsulations into C<sub>84</sub>. *Fullerenes Nanotub. Carbon Nanostruct.* **2016**, *24*, 1–7. [[CrossRef](#)]
38. Slanina, Z.; Uhlík, F.; Nagase, S.; Lu, X.; Akasaka, T.; Adamowicz, L. Computed relative populations of D<sub>2</sub>(22)-C<sub>84</sub> endohedrals with encapsulated monomeric and dimeric water. *ChemPhysChem* **2016**, *17*, 1109–1111. [[CrossRef](#)]
39. Slanina, Z.; Uhlík, F.; Nagase, S.; Akasaka, T.; Adamowicz, L.; Lu, X. Computational comparison of the water-dimer encapsulations into D<sub>2</sub>(22)-C<sub>84</sub> and D<sub>2d</sub>(23)-C<sub>84</sub>. *ECS J. Solid State Sci. Technol.* **2017**, *6*, M3113–M3115. [[CrossRef](#)]
40. Slanina, Z.; Uhlík, F.; Nagase, S.; Akasaka, T.; Adamowicz, L.; Lu, X. A computational characterization of CO@C<sub>60</sub>. *Fullerenes Nanotub. Carbon Nanostruct.* **2017**, *25*, 624–629. [[CrossRef](#)]
41. Slanina, Z.; Uhlík, F.; Nagase, S.; Akasaka, T.; Lu, X.; Adamowicz, L. Cyclic water-trimer encapsulation into D<sub>2</sub>(22)-C<sub>84</sub> fullerene. *Chem. Phys. Lett.* **2018**, *695*, 245–248. [[CrossRef](#)]
42. Slanina, Z.; Uhlík, F.; Adamowicz, L.; Pan, C.; Lu, X. A computational characterization of H<sub>2</sub>O<sub>2</sub>@C<sub>60</sub>. *Fullerenes Nanotub. Carbon Nanostruct.* **2022**, *30*, 258–262. [[CrossRef](#)]
43. Zhang, R.; Murata, M.; Wakamiya, A.; Shimoaka, T.; Hasegawa, T.; Murata, Y. Isolation of the simplest hydrated acid. *Sci. Adv.* **2017**, *3*, e1602833-1–e1602833-6. [[CrossRef](#)] [[PubMed](#)]

44. Zhao, Y.; Truhlar, D.G. The M06 suite of density functionals for main group thermochemistry, thermochemical kinetics, noncovalent interactions, excited states, and transition elements: Two new functionals and systematic testing of four M06-class functionals and 12 other functionals. *Theor. Chem. Acc.* **2008**, *120*, 215–241.
45. Ditchfield, R.; Hehre, W.J.; Pople, J.A. Self-consistent molecular-orbital methods. IX. An extended Gaussian-type basis for molecular-orbital studies of organic molecules. *J. Chem. Phys.* **1971**, *54*, 724–728. [[CrossRef](#)]
46. Schwabe, T.; Grimme, S. Double-hybrid density functionals with long-range dispersion corrections: Higher accuracy and extended applicability. *Phys. Chem. Chem. Phys.* **2007**, *9*, 3397–3406. [[CrossRef](#)] [[PubMed](#)]
47. Moller, C.; Plesset, M.S. Note on an approximation treatment for many-electron systems. *Phys. Rev.* **1934**, *46*, 618–622. [[CrossRef](#)]
48. Boys, S.F.; Bernardi, F. The calculation of small molecular interactions by the difference of separate total energies. Some procedures with reduced errors. *Mol. Phys.* **1970**, *19*, 553–566. [[CrossRef](#)]
49. Slanina, Z.; Lee, S.-L.; Adamowicz, L.; Uhlík, F.; Nagase, S. Computed structure and energetics of La@C<sub>60</sub>. *Int. J. Quantum Chem.* **2005**, *104*, 272–277. [[CrossRef](#)]
50. Basiuk, V.A.; Basiuk, E.V. Noncovalent complexes of I<sub>h</sub>-C<sub>80</sub> fullerene with phthalocyanines. *Fulleren. Nanotub. Carb. Nanostruct.* **2018**, *26*, 69–75. [[CrossRef](#)]
51. Basiuk, V.A.; Tahuilan-Anguiano, D.E. Complexation of free-base and 3d transition metal(II) phthalocyanines with endohedral fullerene Sc<sub>3</sub>N@C<sub>80</sub>. *Chem. Phys. Lett.* **2019**, *722*, 146–152. [[CrossRef](#)]
52. Tahuilan-Anguiano, D.E.; Basiuk, V.A. Complexation of free-base and 3d transition metal(II) phthalocyanines with endohedral fullerenes H@C<sub>60</sub>, H<sub>2</sub>@C<sub>60</sub> and He@C<sub>60</sub>: The effect of encapsulated species. *Diam. Rel. Mat.* **2021**, *118*, 108510-1–108510-5. [[CrossRef](#)]
53. Slanina, Z.; Uhlík, F.; Lee, S.-L.; Adamowicz, L.; Akasaka, T.; Nagase, S. Computed stabilities in metallofullerene series: Al@C<sub>82</sub>, Sc@C<sub>82</sub>, Y@C<sub>82</sub>, and La@C<sub>82</sub>. *Int. J. Quant. Chem.* **2011**, *111*, 2712–2718. [[CrossRef](#)]
54. Frisch, M.J.; Trucks, G.W.; Schlegel, H.B.; Scuseria, G.E.; Robb, M.A.; Cheeseman, J.R.; Scalmani, G.; Barone, V.; Mennucci, B.; Petersson, G.A.; et al. *Gaussian 09, Rev. D.01*; Gaussian Inc.: Wallingford, CT, USA, 2013.
55. Slanina, Z.; Uhlík, F.; Lee, S.-L.; Wang, B.-C.; Adamowicz, L.; Suzuki, M.; Haranaka, M.; Feng, L.; Lu, X.; Nagase, S.; et al. Towards relative populations of non-isomeric metallofullerenes: La@C<sub>76</sub>(T<sub>d</sub>) vs. La<sub>2</sub>@C<sub>76</sub>(C<sub>s</sub>,17490). *Fullerenes Nanotub. Carbon Nanostruct.* **2014**, *22*, 299–306. [[CrossRef](#)]
56. Simon, S.; Bertran, J.; Sodupe, M. Effect of counterpoise correction on the geometries and vibrational frequencies of hydrogen bonded systems. *J. Phys. Chem. A* **2001**, *105*, 4359–4364. [[CrossRef](#)]
57. Legon, A.C.; Millen, D.J.; North, H.M. Experimental determination of the dissociation energies D<sub>0</sub> and D<sub>e</sub> of H<sub>2</sub>O...HF. *Chem. Phys. Lett.* **1987**, *135*, 303–306. [[CrossRef](#)]
58. Slanina, Z. *Contemporary Theory of Chemical Isomerism*; Academia: Prague, Czech Republic; D. Reidel Publ. Comp.: Dordrecht, The Netherlands, 1986; pp. 22–23, 160–164.
59. Slanina, Z.; Uhlík, F.; Lee, S.-L.; Adamowicz, L.; Nagase, S. Computations of endohedral fullerenes: The Gibbs energy treatment. *J. Comput. Meth. Sci. Engn.* **2006**, *6*, 243–250. [[CrossRef](#)]
60. Slanina, Z.; Uhlík, F.; Adamowicz, L. Theoretical predictions of fullerene stabilities. In *Handbook of Fullerene Science and Technology*; Lu, X., Akasaka, T., Slanina, Z., Eds.; Springer: Singapore, 2022; pp. 111–179.
61. Akasaka, T.; Nagase, S.; Kobayashi, K.; Walchli, M.; Yamamoto, K.; Funasaka, H.; Kako, M.; Hoshino, T.; Erata, T. <sup>13</sup>C and <sup>139</sup>La NMR studies of La<sub>2</sub>@C<sub>80</sub>: First evidence for circular motion of metal atoms in endohedral dimetallofullerenes. *Angew. Chem. Int. Ed.* **1997**, *36*, 1643–1645. [[CrossRef](#)]
62. Slanina, Z.; Uhlík, F.; Feng, L.; Akasaka, T.; Lu, X.; Adamowicz, L. Calculations of the Lu<sub>3</sub>N@C<sub>80</sub> Two-Isomer Equilibrium. *Fullerenes Nanotub. Carbon Nanostruct.* **2019**, *27*, 382–386. [[CrossRef](#)]
63. Slanina, Z. Some aspects of mathematical chemistry of equilibrium and rate processes: Steps towards a completely non-empirical computer design of syntheses. *J. Mol. Struct. (Theochem)* **1989**, *185*, 217–228. [[CrossRef](#)]
64. Curtiss, L.A.; Raghavachari, V.; Redfern, P.C.; Rassolov, V.; Pople, J.A. Gaussian-3 (G3) theory for molecules containing first and second-row atoms. *J. Chem. Phys.* **1998**, *109*, 7764–7776. [[CrossRef](#)]

**Disclaimer/Publisher's Note:** The statements, opinions and data contained in all publications are solely those of the individual author(s) and contributor(s) and not of MDPI and/or the editor(s). MDPI and/or the editor(s) disclaim responsibility for any injury to people or property resulting from any ideas, methods, instructions or products referred to in the content.